

Short Review

Materials for Enhanced Dye-sensitized Solar Cell Performance: Electrochemical Application

Suriati Suhaimi¹, Mukhzeer Mohamad Shahimin¹, Z.A. Alahmed², J. Chyský³, A. H. Reshak^{4,5,*}

¹Semiconductor Photonics and Integrated Lightwave System (SPILS), Tun Abdul Razak Laser Laboratory (TAReL), School of Microelectronic Engineering (SoME), Universiti Malaysia Perlis (UniMAP), Pauh Putra Main Campus, Jalan Arau-Changlun, 02600 Arau, Perlis, Malaysia

²Department of Physics and Astronomy, King Saud University, Riyadh 11451, Saudi Arabia

³Department of Instrumentation and Control Engineering, Faculty of Mechanical Engineering, CTU in Prague, Technicka 4, 166 07 Prague 6, Czech Republic

⁴New Technologies - Research Centre, University of West Bohemia, Univerzitni 8, 306 14 Pilsen, Czech republic

⁵Center of Excellence Geopolymer and Green Technology, School of Material Engineering, University Malaysia Perlis, 01007 Kangar, Perlis, Malaysia

*E-mail: maalidph@yahoo.co.uk

Received: 21 December 2014 / Accepted: 28 January 2015 / Published: 24 February 2015

This paper reports on an aperçu of materials that enhance the performance of dye-sensitized solar cells (DSSCs). The review indicates progress in DSSCs and a large improvement in the materials used in DSSCs in particular. DSSCs were assembled using different materials for the semiconductor oxide, dye sensitizer and counter electrode. The performance of each material was evaluated based on photoelectrochemical parameters, including the open circuit voltage (V_{oc}), short circuit current (I_{sc}), fill factor (FF) and overall conversion efficiency (η) from the current-voltage curve. This review covers several types of materials that have paved the way for better-performing solar cells and directly influenced the stability and reliability of DSSCs. The new research trend as well as the previous research has been highlighted to examine the key challenges faced in developing the ultimate DSSCs.

Keywords: Dye-sensitized solar cells, semiconductor oxide, dye sensitizer, counter electrode, electrolyte, conversion efficiency, Electrochemical

1. INTRODUCTION

Among sustainable technologies, such as tidal power, solar thermal, hydropower and biomass [1], photovoltaic technology is regarded as the most efficient. In 1954, the first practical photovoltaic cell using diffused silicon p-n junctions was designed at Bell Laboratories, with an efficiency of 6%.

The important means of producing high-efficiency solar cells are reducing reflectance, trapping light in the cell and increasing light absorption [2]. Silicon solar cells have achieved electricity conversion efficiencies ranging from 15% to 20% [3]. However, the high fabrication cost and the usage of toxic chemicals in producing highly purified silicon during the manufacturing process has motivated the search for an environmentally friendly, low-cost solar cell. Dye-sensitized solar cells (DSSCs) have received considerable attention since O'Regan and Grätzel reported a remarkably high conversion efficiency of nearly 10% [4] using nanocrystalline mesoporous TiO₂ film. However, these organic solar cells are still limited to low power conversion efficiencies [5].

DSSCs are photonic devices that convert visible light into electricity and are based on a porous thin film of a wide-bandgap semiconductor oxide modified by dye molecules. The manufacturing cost of DSSCs, which are 3rd-generation solar cells, is approximately 1/3 to 1/5 times that of silicon solar cells [6]. This type of film enhances the light absorption due to its sponge-like characteristics and increased surface area. The nanocrystalline material plays an essential role in electron injection and transport, determining the performance of the DSSCs [7]. The overall conversion efficiency of DSSCs was reported to be proportional to the injection of electrons in wide-bandgap nanostructured semiconductors. To date, the certified efficiency record is approximately 11.1% for a small cell, and large-scale tests have clarified the great need for the commercialization of DSSCs [8]. Thus, DSSCs have numerous advantages over silicon solar cells.

A typical DSSC consists of a transparent conductive oxide (TCO), semiconductor oxide, dye sensitizer, electrolyte and counter electrode. The working electrode is a nanoporous semiconductor oxide that is placed on conducting glass and is separated from the counter electrode by only a thin layer of electrolyte solution. The extension of the photoelectrode dye enables the collection of lower-energy photons [9]. The dye is chemisorbed onto the semiconductor oxide surface. An ideal sensitizer should adsorb a wide range of wavelengths and possess high thermal stability due to its strong binding to the semiconductor oxide. The photoanode of DSSCs is typically constructed using a thick film (~10 μm) of TiO₂ or, less often, ZnO or SnO₂ nanoparticles [10]. The TiO₂ film has a large inherent absorptive surface area for light scattering. One challenge in the fabrication of DSSCs involves the matching of the material band gaps and the structure design for each layer to give the maximum photoelectrochemical output and thereby the maximum conversion efficiency.

2. DSSC STRUCTURE AND WORKING PRINCIPLE

A single layer of dye molecules acts as a light absorber and is interspersed between TiO₂ particles. A drop of liquid electrolyte containing iodide is placed on the film to percolate into the pores of the film to complete the device. Conductive glass that has been coated with a thin catalytic layer of platinum or carbon as a counter electrode is placed on top of the cell, and light is illuminated from the TiO₂ side, as illustrated in Figure 1. A thicker coating of organic dye for solar cells has been tested; however, electric charges do not move easily within most organic materials, and it was reported that an active charge for charge injection is only effective with extremely thin layers. Thus, thick organic films do not transfer photoexcited charges as well as thin films, absorbing all of the light, and a solar cell

made from an interconnected series of thin film layers would be more effective than a cell made from a single thick layer of dye.

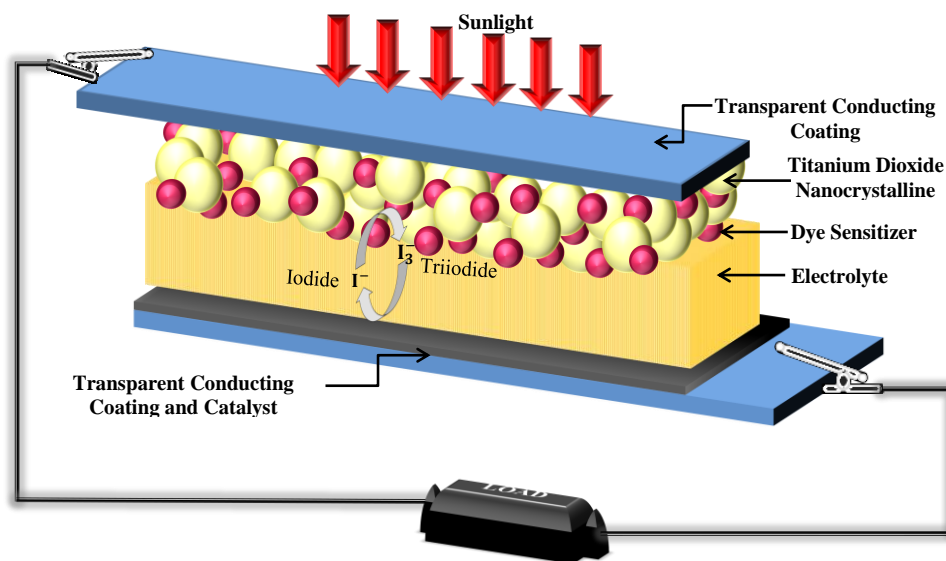


Figure 1. Principle operation of dye-sensitized solar cells (DSSCs) [11] .

The electrons lost by the dye due to the light absorption are quickly replaced by iodide (I^-) in the electrolyte solution, which acts as a mediator. The I^- or triiodide (I_3^-) results from the oxidized mediator, producing an electron catalyst-coated counter electrode after the electron flows through the load [12]. To achieve a reset system capable of repeating the process, energy propagates from the photon to the excited dye photon and then to the TiO_2 layer, conductive glass, load counter electrode, I_3^- , I^- , and finally to the original TiO_2 location [12]. Hence, the electric power generated in a DSSC causes no permanent chemical transformations and is theoretically stable [5].

3. DSSC COMPONENTS

3.1. Transparent Conductive Oxide (TCO)

TCO substrates must be highly transparent (transparency $> 80\%$) to allow the maximum passage of sunlight to the active area [13]. Typically, DSSCs are constructed with two sheets of TCO material as current collectors for the deposition of the semiconductor and catalyst. The TCO material characteristics determine the efficiency of DSSCs [1] due to the efficient charge transfer of electrical conductivity to minimize energy losses. Fluorine tin oxide (FTO, $SnO_2:F$) and indium tin oxide (ITO, $In_2O_3:Sn$) are typical conductive oxide substrates consisting of soda lime glass coated with fluorine tin oxide or indium tin oxide, respectively. The transmittance of ITO films are over 80% in the visible region, with a sheet resistance of approximately $18 \Omega/cm^2$, whereas FTO films exhibit a transmittance of approximately 75% with a sheet resistance of $8.5 \Omega/cm^2$ [13]. Sima et al. conducted a study based

on FTO and ITO glass substrates sintered at 450 °C [14]. They found that upon sintering, the sheet resistance of ITO increased from 18 Ω/cm^2 to 52 Ω/cm^2 , while the sheet resistance of FTO remained constant. The overall conversion efficiencies (η) of DSSCs based on FTO and ITO are approximately 9.4% and 2.4%, respectively. Thus, FTO is strongly recommended for use in DSSC fabrication due to its conduction properties and stable sheet resistance temperature.

Murakami et al. used a polyethylene terephthalate (PET) polymer substrate coated with ITO and obtained a conversion efficiency of approximately 3.8% [15]. Meanwhile, Ito et al. reported an efficiency of 7.8% using polyethylene naphthalate (PEN) [16]. Polymer substrates are attractive alternatives due to their flexibility and low cost. Nevertheless, the use of polymers substrates in DSSCs limits the range of usability due to the requirement of a relatively low fabrication temperature. Another alternative is the use of metals, such as stainless steel, tungsten and titanium, as conducting layer substrates. Jun et al. reported an efficiency of 6.1% [17] using a stainless steel substrate. However, the high cost and corrosion caused by the electrolyte restrict the use of metals as substrates. Creating a new research trend, Braga et al. demonstrated the reliable front contact of cadmium stannate (CTO) and titanium dioxide (TiO_2) deposited entirely by magnetron sputtering. The CTO contact results in a high optical transmittance of approximately 90% along with a sheet resistance of 15 Ω/cm^2 [18].

3.2. Semiconductor Oxide Material

The central part of a DSSC device consists of a thick nanoparticle film that provides a large surface area for light-harvesting absorption molecules to accept electrons from the excited dye [19], such as TiO_2 , ZnO [20], SnO_2 [21], Nb_2O_5 , WO_3 , Ta_2O_5 , CdSe, CdTe, and CdS. These molecules are interconnected to allow electronic conduction [8]. The efficiency of DSSCs depends on the electron transfer rates, which in turn depend on the crystallinity, morphology and surface area of the semiconductor. However, previous research has shown that DSSCs based on ZnO and SnO_2 possess lower efficiency than those based on nanocrystalline TiO_2 [21]-[23] due to the latter's superior morphological and photovoltaic properties [24]. TiO_2 is considered by some to be the most efficient and environmentally benign photocatalyst [25]. Bulk TiO_2 is dominated by three main phases of rutile, anatase and brookite [26]. Anatase TiO_2 is preferred due to its high conduction band edge energy (3.2 eV), which provides chemical stability. In comparison, the conduction band edge energy of rutile is approximately 3 eV. In rutile TiO_2 , electron transport is hindered by the high packing density, and for the same film thickness, anatase-based DSSCs produce a 30% [14] higher short circuit current than rutile-based DSSCs.

Recent trends in research have involved the fabrication of anatase TiO_2 as nanoparticles, nanofibers [27], nanowires [28], hollow spheres [29], hollow hemispheres [30], nanotubes [31], and hierarchical spheres [32] and ellipsoid spheres [33] via solvothermal reactions of titanium *n*-butoxide and acetic acid. The one-dimensional (1D) nanostructure of TiO_2 nanowires has also attracted considerable attention in terms of its application to DSSCs. A novel method has been reported for the synthesis of a TiO_2 nanowire array on FTO glass substrates involving hydrothermal growth [34]. The TiO_2 nanowire with a standard DSSC configuration exhibited a conversion efficiency of approximately

5%, which is considerably higher than the value of 1.2-1.5% attained by ZnO nanowires with lengths of up to $\sim 40 \mu\text{m}$ [34]. Anatase TiO_2 spheres have an overall η of 3.5% with a current density I_{sc} of 17.94%, open circuit voltage V_{oc} of 803 mV and FF of 0.65%. This value of η is much lower than those of DSSCs based on nanoparticles (7.37%), nanofibers (8.15%), and ellipsoid TiO_2 spheres (7.93%) [35]. The improvement of η and I_{sc} by using hierarchical sphere based DSSCs is a result of higher dye loading, improved light scattering ability, faster charge transfer and longer electron lifetime [36] [37]. To produce higher η and I_{sc} , several strategies are used to minimize the recombination. These approaches include the deposition of an insulating layer on the semiconductor electrode. ZnO [38], niobium pentoxide (Nb_2O_5) [39], Al_2O_3 [40], and SiO_2 [41] have been used as an energy barrier to slow the charge recombination due to their insulating character, which reduces the interaction between the electrons injected to the semiconductor and the electrolyte solution [42]. The surface treatment of TiO_2 with TiCl_4 also reduces the charge recombination due to the increasing interfacial charge transfer resistance of TCO/electrolyte interface [43],[44], as demonstrated by Melhem et al. I_{sc} was up to 10% higher when using DSSCs based on an N-doped electrode compared to the pure anatase configuration [45]. This improvement is associated with the electronic and optical properties of the starting nanopowder.

ZnO is an alternative semiconductor oxide material due to its wide band gap, similar to TiO_2 , and its ability to be synthesized simply with different nanostructures. Recently, Keis et al. achieved a conversion efficiency of $\sim 5\%$ under illumination (10 mW/cm^2) with a porous ZnO electrode prepared using the high-pressure compression method and Ru complexes with a carboxylate polypyridine ligand [46]. The advantages of ZnO over TiO_2 include the following [8]: (i) a direct band gap of approximately 3.37 eV, (ii) a higher excitation binding energy (60 meV) compared with TiO_2 (4 meV) and (iii) higher electron mobility ($200 \text{ cm}^2\text{V}^{-1}\text{s}^{-1}$) compared with TiO_2 ($30 \text{ cm}^2\text{V}^{-1}\text{s}^{-1}$). The grain size of ZnO is overly large, and its effective surface area is insufficient; hence, the efficiency of ZnO is low. Therefore, the key to improving the performance of ZnO-based DSSCs is the preparation of a nanoporous ZnO film. Law et al. first reported the use of ZnO nanowire arrays in DSSCs with the aim of replacing the traditional nanoparticle film to increase the electron diffusion length [47]. ZnO nanowire-based DSSCs have been reported to achieve a conversion efficiency of 0.5% and an internal quantum efficiency of 70% due to their high surface area and good connectivity to the electrode. Compared with TiO_2 , the similar electron mobility and conduction band energies of ZnO, in combination with its high excited binding energy, make it a promising candidate for lasing devices and stable room-temperature luminescence [48]. Thus, ZnO nanowire is an alternative candidate for high-efficiency DSSCs.

3.3. Dye Sensitizer

An efficient solar cell sensitizer should adsorb strongly to the surface of the semiconductor oxide via anchoring groups, exhibit intense absorption in the visible part of the spectrum, and possess an appropriate energy level alignment of the dye excited state and the conduction band edge of the semiconductor. The performance of DSSCs mainly depends on the molecular structure of the

photosensitization. Sensitization of the semiconductor in DSSCs has been achieved using numerous chemical compounds, such as phthalocyanines [49]-[51], coumarin 343 [32],[52], carboxylated derivatives of anthracene [53],[54], and porphyrins [55]-[57]. However, the best photosensitization has been attained using metal transition materials [58]. Three classes of dye sensitizers are used in DSSCs: metal complex sensitizers, metal-free organic sensitizers and natural sensitizers.

Ru (II) is the most efficient dye due to its numerous advantageous features, such as good absorption, long excited-state lifetime, and highly efficient metal-to-ligand charge transfer. Ru bipyridyl complexes are excellent photosensitizers due to the stability of the complexes' excited states and the long-term chemical stability of oxidized Ru (III) [59]. The standard dye used in traditional DSSCs is tris(2,2'-bipyridyl-4,4'-carboxylate) ruthenium (II) (N3 dye) [60]. N3 and N719 dyes contain four and two photons, respectively, and were reported to successfully absorb solar light and undergo charge transfer. Another promising candidate is tri(cyanato-2,2',2'',2''-terpyridyl-4,4',4''-tricarboxylate) Ru (II) (black dye), whose response extends approximately 100 nm further into the infrared (IR) region than the response of the N3 dye [60]. Therefore, many researchers have studied Ru bipyridyl complexes as photosensitizers for the reactions of homogeneous photocatalytic and dye-sensitization systems. However, these complexes also have disadvantages, including high cost and the need for sophisticated preparation techniques.

Coumarin is a synthetic organic dye sensitizer obtained from a natural compound found in many plants. Coumarin 343 (C343) is an excellent organic-dye photosensitizer for efficient electron injection into the conduction band of semiconductors. However, the efficiency η for nanocrystalline DSSCs based on the C343 dye is lower than the efficiencies of DSSCs based on Ru-complex photosensitizers because of a lack of absorption in the visible region [52].

Table 1. Various types of plant pigmentation [64].

Pigment Plant	Common Type	Occurrences
Betalains	Betacyanins	Caryophyllales and betaxanthins
	Betaxanthins	some fungi
Carotenoids	Carotenes	Photosynthetic plants and bacteria
	Xanthophylls	Retained from the diet by some birds, fish and crustaceans
Chlorophyll	Chlorophyll	All photosynthetic plants
Flavonoids	Anthocyanin	Widespread and common in plants including angiosperms, gymnosperms, ferns and bryophytes
	Aurones	
	Chalcones	
	Flavonols	
	Proanthocyanidins	

Natural dyes are a viable alternative to expensive organic-based DSSCs. The overall solar energy conversion efficiency of natural dye extracted from pigments containing anthocyanins and carotenoids has been demonstrated to be below 1% [9]. Different parts of the plant, including the

flower petals, fruits, leaves, stems, and roots, typically have different pigments. The advantages of natural dyes are their low cost, easy extraction, non-toxicity and environmentally benign nature [61]. The orange-red Lawsone, red-purple anthocyanin (sensitization of wide bandgap semiconductors) [62] and yellow curcumin are the main components in the natural dyes obtained from these natural products [63]. Plant pigmentation occurs due to the electronic structure of the pigments, and exposure to illuminated light modifies the wavelengths that are either transmitted or reflected by the plant tissue. Table 1 describes the plant pigmentation groups based on a common structure and biosynthesis basis.

Carotenoid pigments are obtained from fruits and plants with distinctive red, orange, and yellow colors and carotenoid-derived aromas. The skeleton of carotenoids may be linear or may contain cyclic end groups, and the major two classes consist of carotenes and their oxygen-generated derivatives, xanthophylls [65]. In addition, carotenoids also provide protection from excess light through the dissipation of energy and free radical detoxification, limiting the damage to the membrane. Flavonoids and their conjugates form a large group of natural products. These components have been observed in many plant tissues, where they can be found inside the cells or on the surfaces of different types of plant organs. The three major classes of flavonoid compounds are anthocyanins, proanthocyanidins, and flavonols. Anthocyanins do not display vivid colors until they are grouped together in acidic vacuoles. Some of the flavonols have protective roles as UV-B filters and function as co-pigments for anthocyanin, especially for special tissues.

The achievement of wide-bandgap semiconductor sensitization using natural pigments is typically attributed to anthocyanin. Anthocyanins compose a major flavonoid group that is responsible for cyanic colors ranging from salmon pink to red and dark violet to dark blue in most flowers, fruits, and leaves of angiosperms [65]. The anthocyanin molecule possesses carboxyl and hydroxyl groups, and it occurs in fruit, leaves, and flowers, where it is responsible for colors ranging from visible red to blue [66]. The bonding causes the electron to move from the anthocyanin molecule to the conduction band of TiO₂. Anthocyanins are often used in organic solar cells due to their ability to absorb light and convert it into electrons. Table 2 describes the performance of various types of natural dyes used as photosensitizers in DSSCs.

Table 2. Photoelectrochemical parameters of DSSCs sensitized by various natural dyes [9],[67] [12],[68]

Dye Sensitizer	Short Circuit Current, J_{sc} (mAcm ²)	Open Circuit Voltage, V_{oc} (V)	Fill Factor	Conversion Efficiency, η
Wormwood	0.196	0.585	0.47	0.538%
Purple Cabbage	0.208	0.660	0.53	0.75%
Turmeric	0.288	0.529	0.48	0.03%
Lemon Leaves	0.272	0.537	0.05	0.05%
Morinda Lucida	0.256	0.440	0.47	0.53%
Wild Silican Prickly Pear	7.320	0.400	0.41	1.21%

Red Turnip	9.500	0.450	0.37	1.70%
Bougainvillea	2.100	0.300	5.7	0.36%

3.4. Electrolyte

Electrolytes are used to regenerate the dye after electron injection into the conduction band of the semiconductor and also act as a charge transport medium for the transfer of positive charge toward the counter electrodes [13]. The liquid electrolyte is based on an organic solvent with a high ionic conductivity and distinctive interfacial contact properties; nevertheless, the leakage and volatility of the solvent affect the long-term performance of DSSCs [65]. Therefore, the electrolyte must have the following characteristics [69]-[70]: (i) high electrical conductivity and low viscosity for faster electron diffusion; (ii) good interfacial contact with the nanocrystalline semiconductor and counter electrode; (iii) no tendency to induce the desorption of the dye from the oxidized surface or the degradation of the dye; and (iv) no absorption of light in the visible region.

A liquid electrolyte consists of a solvent, a redox couple (the most important component), and one or more additives. Other redox couples used include I^-/I_3^- , Br^-/Br_2 [71], $(SCN)_2/SCN^-$, $(SeCN)_2/SeCN^-$ [72]-[73], and bipyridyl cobalt (III/II) complexes [74], which have also been investigated for use in DSSCs [75]. Generally, the liquid electrolyte used in DSSCs contains I^- , I^-/I_3^- , and I_3^- redox ions as a mediator between the TiO_2 photoelectrode and counter electrode. Compared with I^-/I_3^- , the other redox couples exhibit lower DSSC light-to-electricity conversion efficiencies because the energy cannot be matched with the sensitized dye or as a result of their intrinsically low diffusion coefficients in the electrolyte [75].

There are two types of solid-state DSSCs: one using a hole transport material (HTM) as a medium and one using a solid-state electrolyte containing an I^-/I_3^- redox couple as the medium. A solid-state device has recently been described in which the liquid electrolyte based on a porous nanocrystalline oxide film is replaced by a wide-bandgap p-type semiconductor acting as a medium for hole transport [65]. The solid-state device containing a p-type semiconductor has advantages over all solid-state cells due to its easy preparation and higher stability, whereas solar cells occupied with polymer electrolytes exhibit a higher efficiency and have additional future practical applications with proper encapsulation [65]. Organic and inorganic electron HTMs cannot be used as a transport material in DSSCs for practical applications due to their low power conversion efficiencies [75].

3.5. Counter Electrode

Counter electrodes are mainly used to regenerate the electrolyte, with the oxidized electrolyte diffusing towards the counter electrode [13]. The counter electrode transports the electron that arrives from the external circuit back to the redox electrolyte system. Hence, for efficient charge transfer, the counter electrode should exhibit a high catalytic activity and high electrical conductivity [76]. Thus, the catalyst must accelerate the reduction reaction. Based on this consideration, platinum (Pt) is

considered a preferred catalyst. Pt is a superior catalyst for use as a counter electrode for I_3^- reduction because of its high exchange current density, good catalytic activity and transparency. The performance of the counter electrode depends on the method of Pt deposition on TCO substrates, such as the thermal decomposition of hexachloroplatinic in isopropanol [77], electrodeposition [78], sputtering [79], vapor deposition [80], and screen printing.

However, Pt is a rare and expensive metal, and some researchers report that Pt erodes via reaction with I_3^- in the electrolyte to form PtI_4 [81]. The Pt catalytic activity was reported to decrease upon exposure to the dye solution and in the presence of iodide/tri-iodide redox couples [82], likely because its surface is blocked by the adsorbed dye. The major causes of the deactivation of a Pt counter electrode are the alteration of its electrocatalytic properties and the removal of Pt from substrates [77], as demonstrated experimentally. Therefore, carbon, graphene and conductive polymers have also been used as an alternative material for counter electrodes [83].

Carbon is an interesting low-cost alternative because it offers sufficient conductivity and heat resistance in addition to corrosion resistance and electrocatalytic activity for I_3^- reduction [84]. Carbonaceous materials exhibit numerous advantageous features, such as high electronic conductivity, corrosion resistance toward I_3^- reduction, and low cost as substitutes for Pt. In 1996, Kay et al. reported the use of carbon black as a counter electrode, resulting in a conversion efficiency of approximately 6.7% [81]. Josef et al. demonstrated the substitution of a Pt catalyst with a nanocomposite of dry spun carbon multi-walled nanotube (MWNT) sheets with graphene flakes (Gr-F) in a DSSC, reporting an improvement in the catalytic behavior and power conversion efficiency (7.55%) relative to MWNT alone (6.62%) or graphene alone (4.65%) [85]. The latest research by Arman et al. used a Pt-MWCNT counter electrode to obtain a current density J_{sc} of 17.2 mAcm^{-2} , open circuit voltage V_{oc} of 0.690 V and efficiency η of 8.6%, which is the highest photovoltaic performance to date [86]. Table 3 shows the performance of the various counter electrodes.

Table 3. Photoelectrochemical parameters of DSSCs with different counter electrodes [86].

Counter Electrode	Short Circuit Current, J_{sc} (mAcm^{-2})	Open Circuit Voltage, V_{oc} (V)	Fill Factor	Conversion Efficiency, η
Pt	15.3	0.670	0.70	7.2
Pt-MWCNT	17.2	0.690	0.71	8.6
MWCNT	15.1	0.655	0.68	6.7

4. RECOMMENDATIONS

The major challenge in the fabrication and commercialization of DSSCs is the low conversion efficiency and stability of the cell. The degradation of the cell based on dye sensitization, undesirable

electrolyte properties and poor contact with the electrodes are the main causes of the poor performance of DSSCs. To enhance the performance of the DSSCs, several research directions are suggested: (i) improving the dye stability by finding the optimum parameters to slow the dye degradation; (ii) improving the dye structure to absorb more light at longer wavelengths, 780-2500 nm (the near-infrared region, NIR); (iii) improving the morphology of semiconductors to attaining the best electronic conduction to reduce the dark current; (iv) using dye and electrolyte additives to enhance the cell performance; and (v) improving the mechanical contact between the two electrode. Thus, the choice of materials is very important in the fabrication and deployment of DSSCs because the conversion efficiency and stability of the cell do not depend on a single factor alone.

ACKNOWLEDGMENTS

The authors would like to thank their colleagues, technicians and teaching engineers at the Semiconductor Photonics & Integrated Lightwave Systems (SPILS), Tun Abdul Razak Laser Laboratory (TAReL) and Failure Analysis (FA) Lab UniMAP for their helpful advice and discussions, provision of training, and support for the solar cell fabrication. For the author A. H. Reshak, the result was developed within the CENTEM project, reg. no. CZ.1.05/2.1.00/03.0088, cofunded by the ERDF as part of the Ministry of Education, Youth and Sports OP RDI programme and, in the follow-up sustainability stage, supported through CENTEM PLUS (LO1402) by financial means from the Ministry of Education, Youth and Sports under the "National Sustainability Programme I. Computational resources were provided by MetaCentrum (LM2010005) and CERIT-SC (CZ.1.05/3.2.00/08.0144) infrastructures.

References

1. J. Gong, J. Liang and K. Sumathy, *Inorg Chem*, 16 (8) (2012) 5848-5860.
2. A. H. Reshak, M. M. Shahimin, S. Shaari, N. Johan, *Progress in Biophysics and Molecular Biology*, 113 (2) (2013) 327-332.
3. C. D. Grant, A. M. Schwartzberg, G. P. Smestad, J. Kowalik, L. M. Tolbert and J. Z. Zhang, *Inorg Chem*, 522 (1) (2002) 40-48.
4. S. Karuppuchamy, K. Nonomura, T. Yoshida, T. Sugiura and H. Minoura, *Solid State Ionics*, 151 (1) (2002) 19-27.
5. A. H. Reshak, M. M. Shahimin, N. Juhari and R. Vairavan, *Curr. Appl. Phys.*, 13 (9) (2013) 1894-1898.
6. B. O'Regan, and M. Grätzel, *Nature* 353 (1991) 737-740.
7. D. Souza, J. D. Santos, L. O. M. Andrade and A. S. Polo, *Nanoenergy*. Springer Berlin Heidelberg (2013) 49-80.
8. Y. Chergui, N. Nehaoua, D. E. Mekki, *Solar Cells - Dye-Sensitized Devices*, IntechOpen (2011) 49-64.
9. C. Giuseppe, et al., *International journal of molecular sciences*, 11 (1) (2010) 254-267.
10. M. Law, L. E. Greene, J. C. Johnson, R. Saykally and P. Yang, *Nat Mater*, 4 (6) (2005) 455-459.
11. E. Stathatos, *Solar Cells - Dye-Sensitized Devices*, InTech (2011) 471-492.
12. K. F. Moustafa, M. Rekaby, E. T. El Shenawy and N. M. Khattab, *Journal of Applied Sciences Research*, 8 (8) (2012) 4393.
13. U. Mehmood, S. U. Rahman, K. Harrabi, I. A. Hussein and B. V. S. Reddy, *Advances in Materials Science and Engineering*, 2014 (6346) (2014) 1-12.
14. C. Sima, C. Grigoriu and S. Antohe, *Inorg Chem*, 519 (2) (2010) 595-597.

15. T. N. Murakami, Y. Kijitori, N. Kawashima and T. Miyasaka, *Inorg Chem*, 164 (1–3) (2004) 187-191.
16. S. Ito, N. L. C. Ha, G. Rothenberger, P. Liska, P. Comte and S. M. Zakeeruddin, *Chem. Commun.*, 38 (2006) 4004-4006.
17. Y. Jun, J. Kim and M. G. Kang, *Inorg Chem*, 91 (9) (2007) 779-784.
18. A. Braga, C. Baratto, E. Bontempi, P. Colombi and G. Sberveglieri, *Inorg Chem*, 555 (2014) 18-20.
19. M. R. Hoffmann, S. T. Martin, W. Choi and D. W. Bahnemann, *Chem Rev*, 95 (1) (1995) 69-96.
20. O. Lupan, V. Guérin, I. Tiginyanu, V. Ursaki, L. Chow and H. Heinrich, *Inorg Chem*, 211 (1) (2010) 65-73.
21. D. Han, J. Heo, D. Kwak, C. Han, Y. Sung, *Journal of Electrical Engineering Technology*, 4 (1) (2009) 93-97.
22. Y. Fukai, Y. Kondo, S. Mori and E. Suzuki, *Inorg Chem*, 9 (7) (2007) 1439-1443.
23. C. Bauer, G. Boschloo, E. Mukhtar and A. Hagfeldt, *International Journal of Photoenergy*, 4 (1) (2002) 17-20.
24. B. O'Regan and M. Gratzel, *Nature*, 353 (6346) (1991) 737-740.
25. M. I. Baraton, *The Open Nanoscience Journal*, 5 (2011) 64-77.
26. K. Thamaphat, P. Limsuwan and B. Ngotawornchai, *Kasetsart J.(Nat. Sci.)* 42 (5) (2008) 357-361.
27. M. Y. Song, D. K. Kim, K. J. Ihn, S. M. Jo and D. Y. Kim, *Nanotechnology*, 15 (12) (2004) 1861.
28. M. Adachi, Y. Murata, J. Takao, J. Jiu, M. Sakamoto and F. Wang, *J Am Chem Soc*, 126 (45) (2004) 14943-14949.
29. S. C. Yang, D. J. Yang, J. Kim, J. M. Hong, H. G. Kim and I. D. Kim, *Advanced Material*, 20 (5) (2008) 1059-1064.
30. Koo, H- J., et al. *Advanced Materials*, 20 (1) (2008) 195-199.
31. H. Park, W. R. Kim, H. T. Jeong, J. J. Lee, H. G. Kim and W. Y. Choi, *Inorg Chem*, 95 (1) (2011) 184-189.
32. K. D. Seo, H. M. Song, M. J. Lee, M. Pastore, C. Anselmi and F. De Angelis, *Inorg Chem*, 90 (3) (2011) 304-310.
33. Z. S. Wang, H. Kawauchi, T. Kashima and H. Arakawa, *Inorg Chem*, 248 (13–14) (2004) 1381-1389.
34. Q. Zhang and G. Cao, *Nano Today*, 6 (1) (2011) 91-109.
35. J. Y. Liao, J. W. He, H. Xu, D. B. Kuang and C. Y. Su, *J. Mater. Chem.*, 22 (2012) 7910-7918.
36. Y. Saito, S. Kambe, T. Kitamura, Y. Wada and S. Yanagida, *Inorg Chem*, 83 (1) (2004) 1-13.
37. L. Feng, J. Jia, Y. Fang, X. Zhou and Y. Lin, *Inorg Chem*, 87 (2013) 629-636.
38. C. S. Chou, F. C. Chou and J. Y. Kang, *Inorg Chem*, 215–216 (2012) 38-45.
39. T. Y. Cho, K. W. Ko, S. G. Yoon, S. S. Sekhon, M. G. Kang and Y. S. Hong, *Inorg Chem*, 13 (7) (2013) 1391-1396.
40. G R R A Kumara and K Tennakone and V P S Perera and A Konno and S Kaneko and M Okuya, *Inorg Chem*, 34 (6) (2001) 868.
41. T. V. Nguyen, H. C. Lee, M. Alam Khan and O. B. Yang, *Inorg Chem*, 81 (4) (2007) 529-534.
42. E. Palomares, J. N. Clifford, S. A. Haque, T. Lutz and J. R. Durrant, *J Am Chem Soc*, 125 (2) (2002) 475-482.
43. H. Choi, C. Nahm, J. Kim, J. Moon, S. Nam and D. R. Jung, *Inorg Chem*, 12 (3) (2012) 737-741.
44. L. Vesce, R. Riccitelli, G. Soscia, T. M. Brown, A. Di Carlo and A. Reale, *Inorg Chem*, 356 (37–40) (2010) 1958-1961.
45. H. Melhem, P. Simon, J. Wang, C. Di Bin, B. Ratier and Y. Leconte, *Inorg Chem*, 117 (2013) 624-631.
46. P. Suri, M. Panwar and R. M. Mehra, *Materials Science-Poland*, 25 (1) (2001) 04-01.
47. S. Ito, T. N. Murakami, P. Comte, P. Liska, C. Grätzel and M. K. Nazeeruddin, *Thin Solid Films*, 516 (14) (2008) 4613-4619.

48. Q. Peng and Y. Qin, *Nanowires - Implementations and Applications*, IntechOpen (2011).
49. L. Giribabu, V. K. Singh, T. Jella, Y. Soujanya, A. Amat and F. De Angelis, *Inorg Chem*, 98 (3) (2013) 518-529.
50. P. Balraju, M. Kumar, M. Roy and G. Sharma, *Inorg Chem*, 159 (13) (2009) 1325-1331.
51. H. Huang, Z. Cao, X. Li, L. Zhang, X. Liu and H. Zhao, *Inorg Chem*, 162 (24) (2012) 2316-2321.
52. K. Hara, Y. Tachibana, Y. Ohga, A. Shinpo, S. Suga and K. Sayama, *Solar Energy Materials and Solar Cells*, 77 (1) (2003) 89-103.
53. K. Justin Thomas, P. Singh, A. Baheti, Y. C. Hsu, K. C. Ho and J. T. Lin, *Inorg Chem*, 91 (1) (2011) 33-43.
54. J. Mikroyannidis, D. Tsagkournos, S. Sharma, A. Kumar, Y. Vijay and G. Sharma, *Inorg Chem*, 94 (12) (2010) 2318-2327.
55. N. Xiang, W. Zhou, S. Jiang, L. Deng, Y. Liu and Z. Tan, *Inorg Chem*, 95 (4) (2011) 1174-1181.
56. M. K. Panda, K. Ladomenou and A. G. Coutsolelos, *Inorg Chem*, 256 (21-22) (2012) 2601-2627.
57. W. Zhou, B. Zhao, P. Shen, S. Jiang, H. Huang and L. Deng, *Inorg Chem*, 91 (3) (2011) 404-412.
58. K. Kalyanasundaram, *Material Matters*, 4 (4) (2009) 88-90.
59. S. A. Taya, T. M. El-Agez, H. S. El-Ghamri, M. S. Abdel-Latif, *International Journal of Materials Science and Applications*, 2 (2) (2013) 37-42.
60. D. Wei, *International Journal of Molecular Sciences*, 11 (3) (2010) 1103-1113.
61. Q. Dai and J. Rabani, *Inorg Chem*, 26 (4) (2002) 421-426.
62. S. Suhaimi, M. M. Shahimin, I. S. Mohamad and M. N. Norizan, *Advances in Environmental Biology*, 7 (12) (2013) 3617-3620.
63. R. Hemmatzadeh and A. Mohammadi, *Journal of Theoretical and Applied Physics*, 7 (1) (2013) 1-7.
64. D. LEE, *Ann Bot (Lond)*, 96 (7) (2005) 1332-1333.
65. M. R. Narayan, *Renewable and Sustainable Energy Reviews*, 16 (1) (2012) 208-215.
66. R. A. M. Ali and N. Nayan, *International Journal of Integrated Engineering*, 3 (3) (2010) 1-8.
67. H. Chang, M. J. Kao, T. L. Chen, C. H. Chen, K. C. Cho and X. R. Lai, *International Journal of Photoenergy*, 2013 (6346) (2013) 1-8.
68. A. K. Alaba, *Archives of Applied Science Research*, 4 (1) (2012) 419-425.
69. H. Kusama and H. Arakawa, *Inorg Chem*, 85 (3) (2005) 333-344.
70. A. Nogueira, C. Longo and M. A. De Paoli, *Inorg Chem*, 248 (13-14) (2004) 1455-1468.
71. Z.-S. Wang, K. Sayama and S. H., *Journal of Physical Chemistry B*, 109 (47) (2005) 22449-22455.
72. B. V. Bergeron, A. Marton, G. Oskam and G. J. Meyer, *J Phys Chem B*, 109 (2) (2005) 937-943.
73. G. Oskam, B. V. Bergeron, G. J. Meyer and P. C. Searson, *Inorg Chem*, 105 (29) (2001) 6867-6873.
74. S. A. Sapp, C. M. Elliott, C. Contado, S. Caramori and C. A. Bignozzi, *J Am Chem Soc*, 124 (37) (2002) 11215-11222.
75. J. Wu, Z. Lan, S. Hao, P. Li, J. Lin and M. Huang, *Pure and Applied Chemistry*, 80 (11) (2008) 2241-2258.
76. Y. Gao, L. Chu, M. Wu, L. Wang, W. Guo and T. Ma, *Journal of Photochemistry and Photobiology A: Chemistry*, 245 (2012) 66-71.
77. P. N. M. W.-F and G. M., *J. Electrochem. Soc.*, 144 (3) (1997) 876-884.
78. G. Tsekouras, A. J. Mozer and G. G. Wallace, *Journal of the Electrochemical Society*, 155 (7) (2008) K124-K128.
79. X. Fang, T. Ma, G. Guan, M. Akiyama and E. Abe, *Inorg Chem*, 164 (1-3) (2004) 179-182.
80. G. Khelashvili, S. Behrens, C. Weidenthaler, C. Vetter, A. Hinsch and R. Kern, *Inorg Chem*, 511-512 (2006) 342-348.
81. J. Z. Chen, Y. C. Yan and K. J. Lin, *Journal of the Chinese Chemical Society*, 57 (5) (2010) 1180.
82. G. Syrokostas, A. Siokou, G. Leftheriotis and P. Yianoulis, *Solar Energy Materials and Solar Cells*, 103 (2012) 119-127.

83. L. Andrade, H. A. Ribeiro and A. Mendes, *Encyclopedia of Inorganic and Bioinorganic Chemistry*, John Wiley & Sons (2011).
84. A. Kay and M. Grätzel, *Solar Energy Materials and Solar Cells*, 44 (1) (1996) 99-117.
85. J. Velten, A. J. Mozer, D. Li, D. Officer, G. Wallace and R. Baughman, *Nanotechnology*, 23 (8) (2012) 085201.
86. A. Sedghi and H. N. Miankushki, *International Journal of Electrochemical Science*, 9 (2014) 2029-2037.

© 2015 The Authors. Published by ESG (www.electrochemsci.org). This article is an open access article distributed under the terms and conditions of the Creative Commons Attribution license (<http://creativecommons.org/licenses/by/4.0/>).